LETTER

High-efficiency interaction-free measurement with an unbalanced Mach–Zehnder interferometer

IOP Publishing | Astro Ltd
Laser Physics Letters
Laser Phys. Lett. **15** (2018) 065211 (5pp)
https://doi.org/10.1088/1612-202X/aab2b2

Letter

High-efficiency interaction-free measurement with an unbalanced Mach–Zehnder interferometer

Liu Chao[1], Liu Jinhong[1], Zhang Junxiang[1,2] and Zhu Shiyao[1,2,3]

[1] State Key Laboratory of Quantum Optics and Quantum Optics Devices, Institute of Opto-Electronics, Shanxi University, Taiyuan 030006, People's Republic of China
[2] Department of Physics, Zhejiang University, Hangzhou 310027, People's Republic of China
[3] Beijing Computational Science Research Center, Beijing 100084, People's Republic of China

E-mail: junxiang_zhang@zju.edu.cn

Received 8 February 2018
Accepted for publication 28 February 2018
Published 11 May 2018

Abstract

The presence of an object can be detected without the absorption of photons in an interaction-free measurement (IFM) system based on the Zeno effect in chained Mach–Zehnder interferometers (MZIs). In this paper, we propose a scheme with an unbalanced MZI to perform the transmission of two frequency components of input light simultaneously. The two components are separated at two output ports of the MZI, achieving a high probability of asserting the absence of the object. The two final outputs of the MZI can also be extended to perform special information processing via IFM. As a result, this proposal contributes to the improvement of efficiency in interaction-free measurements with a very small number of interferometers for potential practical implementations of quantum information technology.

Keywords: interaction-free measurement, unbalanced Mach–Zehnder interferometer, quantum Zeno effect, information processing

(Some figures may appear in colour only in the online journal)

1. Introduction

No information can be obtained from the quantum state of an object without it being affected by a measurement process. The notion of 'negative result measurement' was first described in 1960 by Renninger: that the state of a quantum system could be determined via the nonobservance of a result [1]. In 1981 a concept of interaction-free measurement (IFM) was proposed by Dicke who analyzed the change of an atomic wave function by the nonscattering of a photon [2]. Elizur and Vaidman proposed an IFM scheme using an optical Mach–Zehnder interferometer (MZI), which detects the presence of an absorbing object without directly interacting with it [3]. Later this kind of counterfactual scheme of gaining information received a lot of attention and has since been widely discussed [4–11]. The idea is that the information about an object can be obtained through the wave–particle duality, in which the interaction between particle and object can be eliminated.

Following on from the scheme of Kwiat *et al* [4], the fraction $\eta = P_{\rm det}/(P_{\rm det} + P_{\rm abs})$ was defined to characterize the efficiency of IFM, where $P_{\rm det}$ is the probability of detecting the presence of an object, and $P_{\rm abs}$ is the probability that the photon be absorbed. An experimental measurement with 50% efficiency was demonstrated using the down-conversion photon pairs in a Michelson interferometer. After that an IFM system made up of a polarization-based MZI structure was considered [12] with $\eta = 2/3$. A polarization-based system was considered for a semitransparent object, for which a IFM of such objects with 100% detection efficiencies can be achievable when the system loss and low quantum efficiency of the

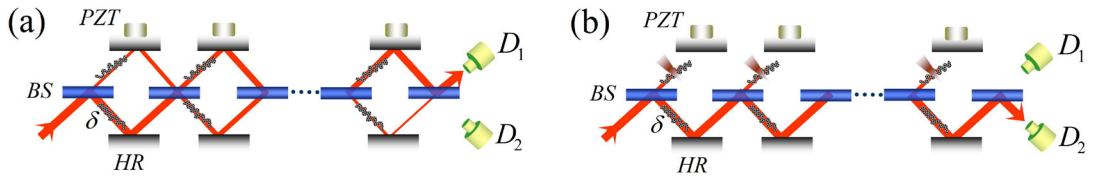

Figure 1. 'Quantum-Zeno-like' IFM scheme: (a) no absorbing objects; (b) with absorbing objects.

photon detectors was negligible [13]. The basic idea of IFM was also applied to detect sensitive quantum objects, such as a single atom [14, 15] and even an electron [16, 17]. Also, the realization of IFM has direct application in interaction-free imaging [18, 19] and quantum information processing [20] through quantum interrogation. In an ideal measurement system, the efficiency can be arbitrarily close to unity if the matter is coherently repeated with interrogations, with the aid of the quantum Zeno effect (QZE) [21–23]; and the experimental demonstrations for improved efficiency of the measurement are presented based on the QZE and IFM [24–26].

In this letter we present a novel approach for achieving high-efficiency IFM, in which a series of MZIs are embedded in an unbalanced MZI [27, 28] with an arm's length difference, and two optical fields are used with a fixed frequency difference as the transmission source. We show the interaction-free effect and demonstrate that a high-efficiency IFM protocol is feasible with a few MZIs for a practical operable system.

2. High-efficiency IFM protocol using an unbalanced MZI

In the protocol of the quantum, Zeno-like IFM suggested by Kwiat, as shown in figure 1, all the beam splitters (BSs) are designed with the same reflectivity $R_N = \cos^2(\pi/2N)$, and the phase difference of the big MZI is set to $\varphi = 2n\pi$ using piezoelectric transducers (PZTs). As a result of interferences in the MZIs, the input light at the lower side of the first BS goes out from the upper side of the last BS, and is detected by the detector D_1, as shown in figure 1(a). On the other hand, if we put absorbing objects in the MZIs, indicated by brown triangles as shown in figure 1(b), the input light is simply reflected by the BSs, and goes out from the lower side of the last BS (at detector D_2). As a result, the detection at D_2 shows the fact that there are objects in the MZIs, and this measurement is interaction-free, as almost no light could be found in the pathway with objects due to the high reflection of the BSs $R_N = \cos^2(\pi/2N)$ when the number N of BSs are large enough.

Being fully interaction-free with the unit efficiency ($\eta = P_{\rm det}/(P_{\rm det} + P_{\rm abs}) = 1$) rests on factors such as having an infinite number of MZIs and no loss in the system. If there is a small number of BSs (e.g. $N < 6$) and an inevitable path loss ($\delta = 10^{-1}$, $\delta = 10^{-2}$ and $\delta = 10^{-3}$) in each MZI for practical measurement, the efficiency decreases rapidly, as shown in figure 2.

Here we present a different scheme of IFM to get a high efficiency with a lower N using an unbalanced MZI. One arm of which includes an $N-1$ number of small chained MZIs (N number of BS_2) for the IFM scheme, and the other has several

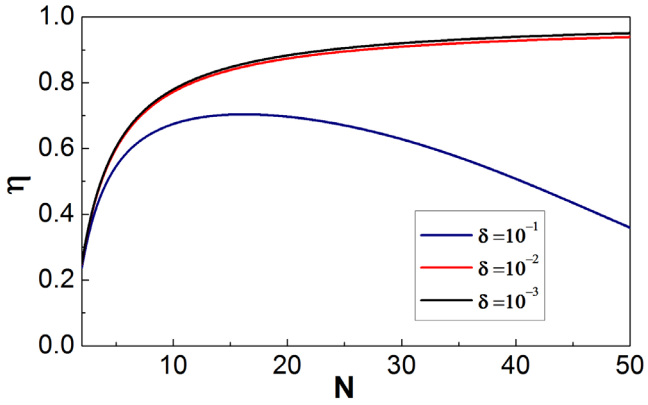

Figure 2. The IFM efficiency η versus N with different path loss.

high-reflectivity mirrors (HRs) to tune the unbalanced arm-length difference ΔL, indicated by the red line, as illustrated in figure 3. Also, a group of balance-loss, optical elements composed of a half-wave plate ($\lambda/2$) and a polarization beam splitter (PBS) is included in the other arm to ensure the parallelism of the two arms of the unbalanced MZIs. The beam splitter BS_1 is designed with a reflectivity $R_{BS_1} = 50\%$. Considering the purpose of IFM, the beam splitter BS_2 is designed with the reflectivity $R_{BS_2} = \cos^2(\pi/2N)$, and the PZTs are used to lock the phase difference of each MZI to zero. With this setup, we take advantage of the image transmission to achieve a high-efficiency IFM for the finite N. The two spatial beams $\hat{a}_{\omega_0+\omega}$ and $\hat{a}_{\omega_0-\omega}$, with a frequency difference of 2ω, are incident to the BS_1 simultaneously. The light intensity distributions in the cross section for $\hat{a}_{\omega_0+\omega}$ and $\hat{a}_{\omega_0-\omega}$ are shown in dot and ring images, respectively. In the case of no absorbing objects (brown triangles), CCD_1 and CCD_2 will capture the same image, which is a superposition of the dot and ring images, and collect one quarter of the original light intensity, respectively. For another case with objects in the arm path of the MZI, CCD_1 and CCD_2 will capture the separate and different images, respectively. As a result, the interaction-free effect can be obtained from all outputs which greatly increase the $P_{\rm det}$. Besides, only the partial optical field transfers to the IFM system through BS1, which greatly decreases the $P_{\rm abs}$. Therefore, the improved measurement system makes it possible for the high-efficiency of the IFM with a very small number of MZIs.

3. Analysis of IFM efficiency with an unbalanced MZI

We divide the improved IFM system into three parts for theoretical analysis, shown in figure 4, which helps us to understand the principle of the setup. The most critical setup is the unbalanced MZI with a path length difference ΔL, as seen in

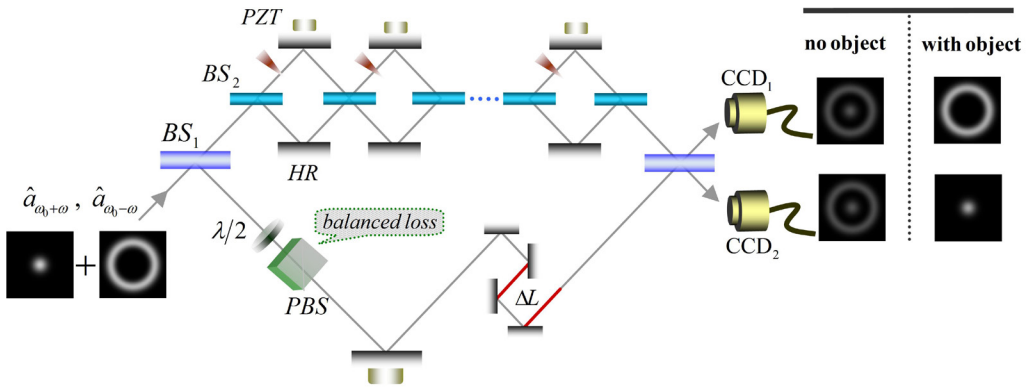

Figure 3. High-efficiency IFM scheme using an unbalanced MZI.

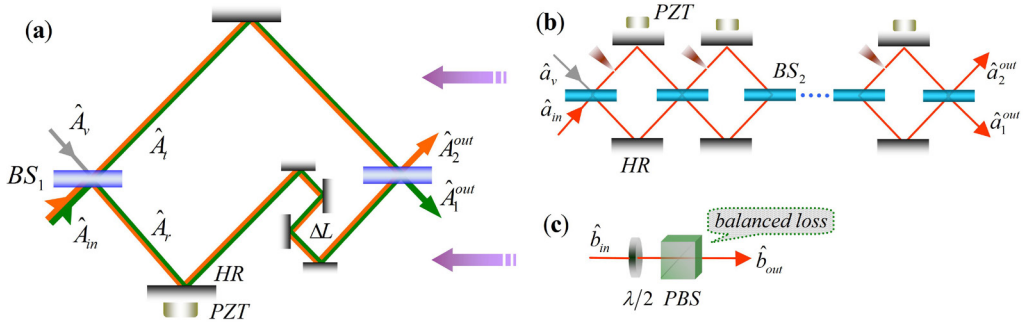

Figure 4. The three optical schemes for high-efficiency IFM: (a) the unbalanced MZI; (b) the IFM system; (c) the balanced optical elements.

figure 4(a). We use the annihilation operator $\hat{A}_{\rm in}$ to represent the input field at $\rm BS_1$, while the vacuum field represented by $\hat{A}_{\rm v}$ is introduced from the other input side of $\rm BS_1$. The output fields are written as $\hat{A}_1^{\rm out}$ and $\hat{A}_2^{\rm out}$. Here the input field has two kinds of frequency: $\omega_0+\omega$ and $\omega_0-\omega$. It can be understood that ω_0 is their central frequency and 2ω is their frequency difference. In the Heisenberg picture, all operators can be written as $\hat{A}(t)=\bar{A}+\delta\hat{A}(t)$ and $\hat{A}^{+}(t)=\bar{A}^{*}+\delta\hat{A}^{+}(t)$ where the functions are relevant to the time, $\bar{A}$ is the classical amplitude of the field and $\delta\hat{A}(t)$ is the fluctuation of the field amplitude. We use a transfer-matrix to describe the optical element. The two beam splitters ($\rm BS_1$) can be expressed by

$$W_{\rm BS_1}=\begin{pmatrix} {\rm i}r_1 & t_1 \\ t_1 & {\rm i}r_1 \end{pmatrix}, \tag{1}$$

where $r_1=\sqrt{2}/2$ and $t_1=\sqrt{2}/2$ are the reflection and transmission amplitudes of the $\rm BS_1$, respectively. The phase shift in one path of the unbalanced MZI can be represented as

$$W_{\varphi}=\begin{pmatrix} {\rm e}^{{\rm i}\varphi} & 0 \\ 0 & 1 \end{pmatrix}, \tag{2}$$

where φ is the phase difference by using PZT to drive the corresponding HR. As a result, the whole transformation process can be expressed as

$$\begin{aligned}\begin{pmatrix} \delta\hat{A}_{\rm r}(t) \\ \delta\hat{A}_{\rm t}(t) \end{pmatrix} &= W_{\rm BS_1}\begin{pmatrix} \delta\hat{A}_{\rm in}(t) \\ \delta\hat{A}_{\rm v}(t) \end{pmatrix}, \quad \begin{pmatrix} \delta\hat{A}_1^{\rm out}(t) \\ \delta\hat{A}_2^{\rm out}(t) \end{pmatrix} \\ &= W_{\rm BS_1}\cdot W_{\varphi}\cdot\begin{pmatrix} \delta\hat{A}_{\rm r}(t-\tau) \\ \delta\hat{A}_{\rm t}(t) \end{pmatrix}, \end{aligned} \tag{3}$$

here τ is the time delay between the two paths. By using the relation of the time and frequency domains in the Fourier transform $\delta\hat{A}(t)\rightarrow\delta\hat{A}(\omega)$, we have

$$\begin{aligned}\delta\hat{A}_{1,\varphi}^{\rm out}(\omega) &= \frac{1}{2}\left[\delta\hat{A}_{\rm in}(\omega)\left(1-{\rm e}^{{\rm i}\varphi+{\rm i}\omega\tau}\right)\right] \\ &+\frac{\rm i}{2}\left[\delta\hat{A}_{\rm v}(\omega)\left(1+{\rm e}^{{\rm i}\varphi+{\rm i}\omega\tau}\right)\right], \end{aligned} \tag{4}$$

$$\begin{aligned}\delta\hat{A}_{2,\varphi}^{\rm out}(\omega) &= \frac{\rm i}{2}\left[\delta\hat{A}_{\rm in}(\omega)\left({\rm e}^{{\rm i}\varphi+{\rm i}\omega\tau}+1\right)\right] \\ &+\frac{1}{2}\left[\delta\hat{A}_{\rm v}(\omega)\left({\rm e}^{{\rm i}\varphi+{\rm i}\omega\tau}-1\right)\right]. \end{aligned} \tag{5}$$

We note that when setting the phase difference $\varphi=(2n+1)\pi/2$, $\omega\tau=(2n+1)\pi/2$, the result for the propagation of the optical field is

$$\delta\hat{A}_{1,\pi/2}^{\rm out}(\omega)=\delta\hat{A}_{\rm in}(\omega),\quad \delta\hat{A}_{2,\pi/2}^{\rm out}(-\omega)={\rm i}\delta\hat{A}_{\rm in}(-\omega), \tag{6}$$

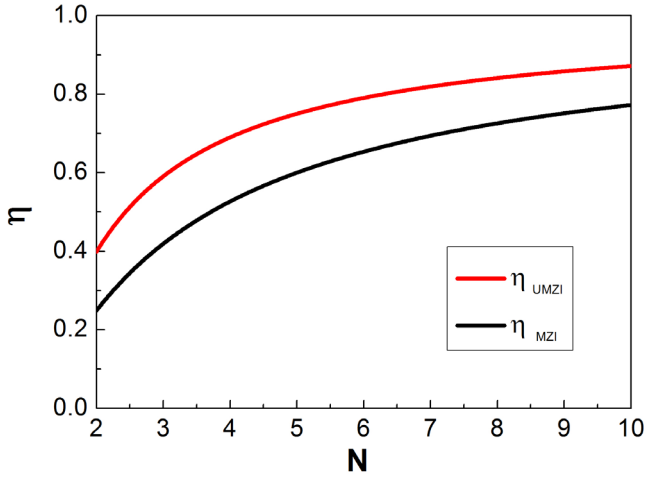

Figure 5. The efficiencies η_{UMZI} and η_{MZI} versus N with $\delta_{\mathrm{path}} = 0.01$.

$$\delta\hat{A}^{\mathrm{out}}_{1,\pi/2}(-\omega) = \mathrm{i}\delta\hat{A}_{\mathrm{v}}(-\omega), \quad \delta\hat{A}^{\mathrm{out}}_{2,\pi/2}(\omega) = -\delta\hat{A}_{\mathrm{v}}(\omega). \tag{7}$$

It can be noticed that the input field with two different frequencies will be separated into two independent spatial lights. If the phase difference is locked to $\varphi = -\pi/2$ using the PZT, the result for the propagation of the optical field is reversed.

Through the above theoretical analysis, we can obtain the specific value of the path length difference $\Delta L = (2n+1)\pi \cdot c/2\omega$ (c is velocity of light) to separate two beams with a different frequency.

Next we analyze the IFM system, which is the upper arm of the unbalanced MZI as shown in figure 4(b). The input field $\hat{a}_{\mathrm{in}}$ is incidental from the first BS_1, while the vacuum field $\hat{a}_{\mathrm{v}}$ is incidental from the other end, and the absorbing objects (brown triangle) are placed in the upper part of the MZIs. Now we still use the transfer-matrix method to analyze the outputs passing through the chain of MZIs. The beam splitters (BS_2) can be expressed by

$$W_{\mathrm{BS}_2} = \begin{pmatrix} r_2 & -t_2 \\ t_2 & r_2 \end{pmatrix}, \tag{8}$$

where $r_2 = \cos(\pi/2N)$ and $t_n = \sin(\pi/2N)$ are the reflection and transmission amplitudes of the BS_2, respectively, and N is the number of the BS_2. The spatial transfer matrix of two adjacent BS_2s can be represented as

$$W_{\phi} = \begin{pmatrix} \mathrm{e}^{\mathrm{i}\phi} & 0 \\ 0 & \sqrt{1-\delta_{\mathrm{abs}}} \end{pmatrix}, \tag{9}$$

where ϕ is the phase difference of each MZI using PZTs, and δ_{abs} is used to describe the absorption of the light field. Note that W_{ϕ} has a different form for the two cases ($\delta_{\mathrm{abs}} = 1$ with objects, and $\delta_{\mathrm{abs}} = 0$ without objects). We use the column vector $(\hat{a}_{\mathrm{in}}, \hat{a}_{\mathrm{v}})^{\mathrm{T}}$ to represent the input state and the output state can be written as $(\hat{a}^{\mathrm{out}}_1, \hat{a}^{\mathrm{out}}_2)^{\mathrm{T}} = W^{\mathrm{total}}(\hat{a}_{\mathrm{in}}, \hat{a}_{\mathrm{v}})^{\mathrm{T}}$, here W^{total} is the whole transformation matrix of the IFM device, which has a different form based on the two cases. As a result, the whole transformation process can be expressed as

$$W^{\mathrm{total}} = (W_{\mathrm{BS}_2} \cdot W_{\phi})^{N-1} \cdot W_{\mathrm{BS}_2}. \tag{10}$$

The values of the output intensity relative to the initial intensity for the two outputs $\hat{a}^{\mathrm{out}}_1$ and $\hat{a}^{\mathrm{out}}_2$ can be calculated according to the modular square of the matrix element W^{total}_{11} and W^{total}_{21}.

If there are no objects in the MZIs, and the phase difference of each MZI is set to be $\phi = 2n\pi$, we get the values $\left|W^{\mathrm{total}}_{11}\right|^2 = 0$ and $\left|W^{\mathrm{total}}_{21}\right|^2 = 1$, which means all the light will exit from the upper port of the last BS_2, and no light enter the unbalanced MZI. For the other case with objects, we get the values $\left|W^{\mathrm{total}}_{11}\right|^2 = \cos^{2N}(\pi/2N)$ and $\left|W^{\mathrm{total}}_{21}\right|^2 = 0$, which means most of the light-field will enter the unbalanced MZI after the $(N-1)$th loop, and no light exit from the upper port of the last BS_2. The result demonstrates that the unbalanced MZI can be operated for the presence of objects, and destroyed for the absence of objects.

Furthermore, we consider the influence of the different intensities on the measurement between two arms of the unbalanced MZI resulting from the chained MZIs of the IFM, which leads to the incomplete interference of the two beams. Therefore, we add the adjustable loss δ_{adj}, using a half-wave plate ($\lambda/2$), and a PBS in the bottom path of the unbalanced MZI, as shown in figure 4(c). The input field $\hat{b}_{\mathrm{in}}$ passes through the optical element with the compensation-based loss $\delta_{\mathrm{adj}} = 1 - \cos^{2N}(\pi/2N)$, therefore the intensity of the output field $\hat{b}_{\mathrm{out}}$ can be obtained with the equality of intensity for the light field $\hat{a}^{\mathrm{out}}_1$.

According to the discussion above, a high-efficiency IFM scheme using an unbalanced MZI is feasible; the P_{det} and P_{abs} are as follows:

$$P_{\mathrm{det}} = (1-\delta_{\mathrm{path}})^{N-1} \cdot \cos^{2N}(\pi/2N), \tag{11}$$

$$P_{\mathrm{abs}} = \frac{1}{2}\sum_{l=0}^{N-1} \cos^{2l}(\pi/2N) \cdot (1-\delta_{\mathrm{path}})^{1} \cdot \sin^{2}(\pi/2N), \tag{12}$$

where δ_{path} is the unavoidable path loss of each MZI. During the measurement we adjusted the δ_{adj} to be $1-(1-\delta_{\mathrm{path}})^{N-1} \cdot \cos^{2N}(\pi/2N)$. In figure 5, we plot the IFM efficiency η as a function of N with $\delta_{\mathrm{path}} = 0.01$. It can be seen that the efficiency $\eta_{\mathbf{UMZI}}$ of the unbalanced MZI (red curve) with the IFM system is higher than the $\eta_{\mathbf{MZI}}$ of the MZIs (black curve) under a finite number of beam splitters. For example, although we could obtain a $\eta_{\mathrm{UMZI}} = 80\%$ with $N = 6$, it is much larger than the corresponding efficiency $\eta_{\mathrm{MZI}} = 65\%$. High efficiency is necessary in the practical setup for potential application.

4. Conclusions

We have presented a high-efficiency IFM system in which the number of interferometers is considered to be small for practical applications. We also proposed an optimum model of IFM with an unbalanced MZI, in which the spatial image information can be read out simultaneously. We have discussed the

light field transmission in the system through the transfer-matrix method and found that the spatial beams with different frequencies go out from two outputs with almost no light absorbed, thus the probability of detecting the presence of objects is substantially improved. It is thus concluded that a high-efficiency IFM could be achieved with a very small number of interferometers. The design concept will be beneficial for detecting the presence of sensitive or perishable devices in practical applications.

Acknowledgments

This work is supported by National Natural Science Foundation of China (11574188), National Natural Science Foundation of China (11634008), project support by the Program of State Key Laboratory of Quantum Optics and Quantum Optics Devices (No: KF201702), research fund for the doctoral program of higher education of China (20131401110013) and Zhejiang Provincial Natural Science Foundation of China under Grant (No: LD18A040001).

References

[1] Renninger M 1960 *Z. Phys.* **158** 417 [This is written in German, a relatively clear discussion of the paper in English is given in Cramer J G 1986 *Rev. Mod. Phys.* **58** 647]
[2] Dicke R H 1981 Interaction-free quantum measurements: a paradox? *Am. J. Phys.* **49** 925
[3] Elitzur A and Vaidman L 1993 Quantum mechanical interaction-free measurements *Found. Phys.* **23** 987
[4] Kwait P G, Weinfurter H, Herzog T, Zeilinger A and Kasevich M A 1995 Interaction-free measurement *Phys. Rev. Lett.* **74** 4763
[5] White A G, Mitchell J R, Nairz O and Kwait P G 1998 'Interaction-free' imaging *Phys. Rev.* A **58** 605
[6] Hafner M and Summhammer J 1997 Experiment on interaction-free measurement in neutron interferometry *Phys. Lett.* A **235** 563
[7] Paul H and Pavicic M 1997 Nonclassical interaction-free detection of objects in a monolithic total-internal-reflection resonator *J. Opt. Soc. Am.* B **14** 1275
[8] Karlsson A, Bjork G and Forsberg E 1998 'Interaction' (energy exchange) free and quantum nondemolition measurements *Phys. Rev. Lett.* **80** 1198
[9] Paraoanu G S 2006 Interaction-free measurements with superconducting qubits *Phys. Rev. Lett.* **97** 180406
[10] Thomas S, Kohstall C, Kruit P and Hommelhoff P 2014 Semi-transparency in interaction-free measurements *Phys. Rev.* A **90** 053840
[11] Zhou Y and Yung M H 2017 Interaction-free measurement as quantum channel discrimination *Phys. Rev.* A **96** 062129
[12] Kwait P G, Weinfurter H, Herzog T, Zeilinger A and Kasevich M A 1996 *Proceedings of the Seventh Rochester Conference on Coherence and Quantum Optics,University of Rochester, 1995* ed E Wolf (New York: Plenum)
[13] Jang J S 1999 Optical interaction-free measurement of semi-transparent objects *Phys. Rev.* A **59** 2322
[14] Volz J, Gehr R, Dubois G, Estève J and Reichel J 2011 Measurement of the internal state of a single atom without energy exchange *Nature* **475** 210
[15] Li Z H, Al-Amri M and Zubairy S 2015 Direct counterfactual transmission of a quantum state *Phys. Rev.* A **92** 052315
[16] Putnam W P and Yanik M F 2009 Noninvasive electron microscopy with interaction-free quantum measurements *Phys. Rev.* A **80** 040902
[17] Chirolli L, Strambini E, Giovannetti V, Taddei F, Piazza V, Fazio R, Beltram F and Burkard G 2010 Electronic implementations of interaction-free measurements *Phys. Rev.* B **82** 045403
[18] Kruit P *et al* 2016 Designs for a quantum electron microscope *Ultramicroscopy* **164** 31
[19] Inoue S and Björk G 2000 Experimental demonstration of exposure-free imaging and contrast amplification *J. Opt.* B **2** 338
[20] Hosten O, Rakher M T, Barreiro J T, Perer N A and Kwait P G 2006 Counterfactual quantum computation through quantum interrogation *Nature* **439** 949
[21] Misra B and Sudarshan E C G 1977 The Zeno's paradox in quantum theory *J. Math. Phys.* **18** 756
[22] Peres A 1980 Zeno paradox in quantum theory *Am. J. Phys.* **48** 931
[23] Agarwal G S and Tewari S P 1994 An all-optical realization of the quantum Zeno effect *Phys. Lett.* A **185** 139
[24] Ma X S, Guo X, Schuck C, Fong K Y, Jiang L and Tang H X 2014 On-chip interaction-free measurements via the quantum Zeno effect *Phys. Rev.* A **90** 042109
[25] Kwiat P G, White A G, Mitchell J R, Nairz O, Weihs G, Weinfurter H and Zeilinger A 1999 High-efficiency quantum interrogation measurements via the quantum Zeno effect *Phys. Rev. Lett.* **83** 4725
[26] Tsegaye T, Goobar E, Karlsson A, Björk G, Loh M Y and Lim K H 1998 Efficient interaction-free measurements in a high-finesse interferometer *Phys. Rev.* A **57** 3987
[27] Glöckl O, Andersen U L, Lorenz S, Silberhorn Ch, Korolkova N and Leuchs G 2004 Sub-shot-noise phase quadrature measurement of intense light beams *Opt. Lett.* **29** 1936
[28] Huntington E H, Milford G N and Robilliard C 2005 Demonstration of the spatial separation of the entangled quantum sidebands of an optical field *Phys. Rev.* A **71** 041802